Eur. Phys. J. B **14**, 115–124 (2000)

**THE EUROPEAN PHYSICAL JOURNAL B**

EDP Sciences


# Photo-excitation from dia- to ferri-magnetism in a Rb–Co–hexacyanoferrate Prussian blue analogue

A. Goujon[1], O. Roubeau[1], F. Varret[1,a], A. Dolbecq[2], A. Bleuzen[2], and M. Verdaguer[2]

[1] Laboratoire de Magnétisme et d'Optique, CNRS-Université de Versailles[b], 45 avenue des États-Unis, 78035 Versailles Cedex, France

[2] Laboratoire de Chimie Inorganique et Matériaux Moléculaires, CNRS-Université Pierre et Marie Curie[c], 4 place Jussieu, 75252 Paris Cedex 05, France

Received 12 March 1999 and Received in final form 11 December 1999

**Abstract.** We studied the photo-excitation process, the relaxation of the photo-excited state towards the stable state, and the photo-induced magnetic properties of the Prussian blue analogue $Rb_{0.52}Co\ [Fe(CN)_6]_{0.84}$, 2.3 $H_2O$. Magnetic, Mössbauer and reflectivity measurements have been performed during and after illumination. The efficiency of the photo-excitation device is maximum at $\lambda \cong 700-750$ nm. The process, however, is severely hindered by bulk absorption of the light; it is rapidly completed at the surface of the sample and then proceeds slowly in the bulk. Under the effect of photo-excitation the system turns from a dia- to a ferri- magnet, with a $T_C$ value $\geq 21$ K, indicative of the transformation of the material due to the following optical electron transfer: $Fe^{II}(LS) + Co^{III}(LS) \rightarrow Fe^{III}(LS) + Co^{II}(HS)$ Thermal relaxation towards the stable electronic state is observed in the 95–110 K temperature interval, obeying a self-accelerated kinetics. At low temperature, a weak, non-exponential, relaxation is detected. These features are discussed in terms of co-operative effects in the frontal process of photo- excitation. The peculiarities of a photo-excited state created below the magnetic ordering temperature are discussed. A metastable magnetic state has been observed in low fields, denoted "Raw Photo-Induced State" (RPI), with a magnetization curve in-between the field-cooled and zero-field-cooled curves.

**PACS.** 75.50.Xx Molecular magnets – 78.40.Ha Other nonmetallic inorganics – 82.20.Mj Nonequilibrium kinetics

## 1 Introduction

For the past decade, the synthesis of molecule-based magnets with high Curie temperature has attracted a growing interest because:

(i) the magnetic ordering temperature or Curie temperature $T_C$ has recently been increased to room temperature in the Prussian blue analogue $V[Cr(CN)_6]_{0.86}.2.8H_2O$ [1];
(ii) spectacular photomagnetic effects have been observed in the $KCo[Fe(CN)_6]$ and $RbCo[Fe(CN)_6]$ series [2,3].

The Prussian blue analogues are formed by three-dimensional association of metallic cations, $A^{l+}$, Lewis acids, and hexacyanometalates $[B(CN)_6]^{k-}$ Lewis bases. They have the rock salt structure with $[B(CN)_6]$ units at the vertices of the unit cell and at the center of the faces and A cations in the octahedral sites. Alkali cations $C^I$ can be inserted in the tetrahedral sites and various stoichiometries are thus obtained, according to the A-cation valence and to the nature and amount of alkali cations. Figure 1 shows the structure of the two extreme stoichiometries $A^{II}_3[B^{III}(CN)_6]_2$ (a) and $C^IA^{II}[B^{III}(CN)_6]$ (b) available for a divalent A cation and a trivalent B ion. The cobalt-iron analogue (A = Co, B = Fe) is not interesting for its potential application as a room temperature ferromagnet ($T_C$ = 16 K) but for the sensitivity of its magnetic properties to light irradiation: Hashimoto *et al.* have shown that the magnetization of $K_{0.14}Co[Fe(CN)_6]_{0.71}$ is enhanced by red light illumination and partly restored by blue light irradiation [2]. The electronic states of cobalt iron cyanides are now better characterized. We have shown that $Co_3[Fe(CN)_6]_2$ consists of $Fe^{III}(t^5_{2g}$, low spin, $S = 1/2)$ – $CN-Co^{II}(t^5_{2g}e^2_g$, $S = 3/2)$ magnetic pairs. Indeed, with such a $Co_3Fe_2$ stoichiometry, $Fe(CN)_6$ entities are missing, water molecules fill the vacancies, some co-ordinate to cobalt(II), the surrounding of which is mainly $[Co^{II}(NC)_4(H_2O)_2]$, *i.e.* in a weak ligand field. The insertion of alkali cation modifies the stoichiometry, suppresses the $Fe(CN)_6$ vacancies, changes the cobalt surrounding to $[Co^{II}(NC)_6]$, which is

[a] e-mail: fvarret@physique.uvsq.fr
[b] Unité Mixte 8634
[c] Unité Associée 7071

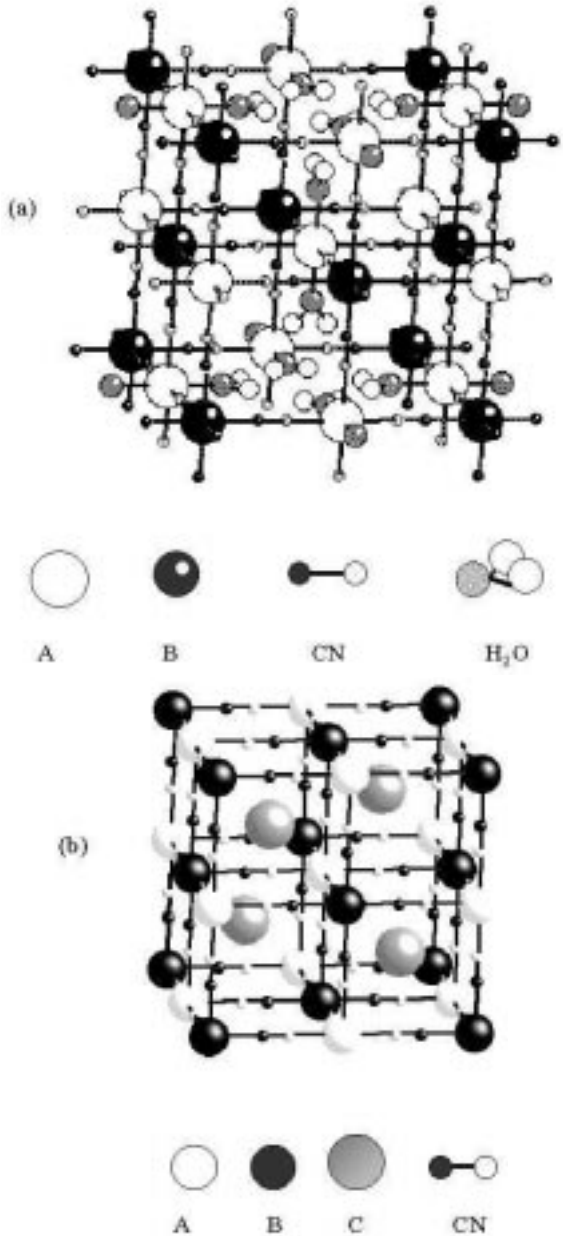


**Fig. 1.** Schematic structures of (a) $A_3^{II}[B^{III}(CN)_6]_2$ and (b) $C^IA^{II}[B^{III}(CN)_6]$.

enough to produce an increase of the ligand field around the cobalt ion and to stabilise a low spin cobalt(II) electronic configuration. An internal redox reaction between $Co^{II}$ and $Fe^{III}(CN)_6$ is therefore induced and results in the formation of $Fe^{II}(t_{2g}^6, S = 0)$ – CN–$Co^{III}(t_{2g}^6, S = 0)$ diamagnetic pairs [4]. In $K_{0.14}Co[Fe(CN)_6]_{0.71}$ only a small amount of potassium is inserted, the electron transfer affects a few Co–Fe pairs and the main part of the cobalt ions remain Co(II). The red illumination operates on the few diamagnetic $Fe^{II}$–CN–$Co^{III}$ pairs, an electron is transferred back from iron to cobalt, restoring the $Fe^{III}(t_{2g}^5, S = 1/2)$–CN–$Co^{II}(t_{2g}^5e_g^2, S = 3/2)$ magnetic pairs.

The number of photo-excitable pairs should therefore be enhanced in a compound with a Fe/Co ratio closer to 1. To reach this stoichiometry alkali cations with larger radii, such as rubidium or cesium, which fit better the size of the tetrahedral cavities, have to be used. We thus report here the synthesis of the Prussian blue analogue $Rb_{0.52}Co[Fe(CN)_6]_{0.84}$ and the investigation of its photomagnetic properties.

Preliminary measurements have been published in [3–5].

## 2 Experimental part

The synthesis of $Rb_{0.52}Co[Fe(CN)_6]_{0.84}$ is similar to that of the cesium compound previously described [6]: $Rb_{1.5}K_{1.5}Fe(CN)_6$ was first synthesized by addition of a 2 ml aqueous solution of RbCl (1.209 g, $10^{-2}$ mol) to a 3 ml aqueous solution of $K_3[FeCN)_6]$ (1.646 g, $5 \times 10^{-3}$ mol). The precipitate was filtered and dried. Analysis: calcd. for $Rb_{1.5}K_{1.5}Fe(CN)_6$ (found): Rb 32.16 (31.83), K 14.71 (14.58), Fe 14.01 (13.45), C 18.07 (18.48), N 21.07 (21.40). A 500 ml aqueous solution of $Co(NO_3)_{2.6}H_2O$ (2.910 g, $10^{-3}$ mol) was then added dropwise under vigorous stirring to a 50 ml aqueous solution of $Rb_{1.5}K_{1.5}Fe(CN)_6$ (3.987 g, $10^{-3}$ mol). The resulting precipitate was isolated by centrifugation, washed three times with 50 ml of water and dried under vacuum. Anal. (calcd.) for $Rb_{0.52}Co[Fe(CN)_6]_{0.84}2.3\,H_2O$: Rb 13.25 (13.02), Fe 13.99 (13.43), Co 17.57 (17.11), C 18.03 (18.57), N 21.04 (21.48), H 1.79 (1.34).

The material was characterized by powder X-ray diffraction and IR spectroscopy. Elemental analysis shows that the expected stoichiometry $Rb_1Co[Fe(CN)_6]_1$ is not reached, probably because rubidium is not large enough to stay inside the tetrahedral cavities and has been washed out during the purification steps. Attempts to incorporate a larger amount of Rb, by adding a large excess of RbCl during the synthesis, failed. IR spectral measurements in the region from 2000 $cm^{-1}$ to 2200 $cm^{-1}$, sensitive to the CN stretching vibration, show a strong peak at 2126 $cm^{-1}$ and a shoulder at 2090 $cm^{-1}$. The peak at 2126 $cm^{-1}$ is due to the stretching of CN in $Fe^{II}$–CN–$Co^{III}$ pairs while the shoulder at 2090 $cm^{-1}$ can be assigned to the stretching of CN in $Fe^{II}$–CN–$Co^{II}$ pairs [4]. Furthermore the X-ray powder pattern is consistent with a cubic structure. The value of the unit cell parameter (9.92 Å), compared to 10.25 Å for the $Co_3[Fe(CN)_6]_2$ compound [4], indicates that the electron transfer occurred between Fe(III) and Co(II). The contraction of the Co–NC bond distance, from $Co^{II}$ (high spin) – NC to $Co^{III}$ (low spin) – NC, is indeed responsible for the shrinking of the unit cell [4]. As the Fe/Co ratio is slightly smaller than 1, a small part of the cobalt ions remain Co(II). However, this structural change associated with the electron transfer and the spin conversion of some cobalt ions, does not require that all Co ions become Co(III). The detailed formula of the compound,

expressing the oxidation states of all the ions, can be expressed as $Rb^{I}_{0.52}Co^{II}_{0.16}Co^{III}_{0.84}[Fe^{II}(CN)_6]_{0.84}$.

We have studied several samples, either polycrystalline, or embedded in polymeric matrix; the latter are supposed to retain the stoichiometry of the starting solid complex. The data are currently given for the polycrystalline samples, unless the reverse is mentioned. The magnetization curves have been recorded in a SQUID magnetometer (Quantum Device MPMS5) operating in the alternative mode, equipped with an Y-shaped optical fiber, made of multiwire silica. The two flexible ends of the fiber were connected to (i) a broadband source of light (tungsten halogen lamp, 100 W), through interferential filters (100 nm bandwidth) and (ii) the photodiode at the input of the reflectivity recording system [5–7]. A cut-off filter $\lambda > 665$ nm provided, with the source and fibers, a large intensity in the range [665−1000] nm.

The Mössbauer cryostat was a standard bath cryostat (Oxford MD300); the sample holder was designed to receive the same optical fiber, with an aluminized mylar mirror, oriented at 45° in front of the sample. The distance between the end of the fiber and the sample was typically 1.5 cm in the Mössbauer system. It was only $\sim 1$ mm in the magnetometer, thanks to a short rod of silica (optical fiber) inserted between the sample and the end of the fiber. This additional rod was needed because the stainless steel tube, which houses the fiber, is not a perfect diamagnet. The energy flux received by the sample was typically in the range 1−100 mW/cm$^2$.

## 3 The photo-excitation process

The photo-excitation process in the analogous system $K_{0.2}Co_{1.4}[Fe(CN)_6]$, 3.6 $H_2O$, was previously described by Sato *et al.* [2], in terms of an optical electron transfer from $Fe^{II}$ to $Co^{III}$, associated with a change of the resulting $Co^{II}$ spin state. This was summarized through the following reaction equation:

$$Fe^{II}(LS) + Co^{III}(LS) \rightarrow Fe^{III}(LS) + Co^{II}(HS) \quad (1)$$
$$S = 0 + S = 0 \rightarrow S = 1/2 + S = 3/2.$$

Accounting for the actual stoichiometry of the sample, the complete photo- transformation of the system should be written as:

$$0.16\ Co^{II} + 0.84\ Co^{III} + 0.84\ Fe^{II} \rightarrow Co^{II} + 0.84\ Fe^{III}. \quad (2)$$

The results we report here confirm the validity of this mechanism, and show it takes place, almost quantitatively, in the surface part of the sample directly submitted to the light beam.

Typical Mössbauer spectra are shown in Figure 2, with the fitted hyperfine parameter values listed in Table 1. The sample was a thin foil of polymer-embedded $Rb_{0.52}Co[Fe(CN)_6]_{0.84}$, kept at 47 K (low-pressure liquid nitrogen). Before illumination, within the experimental accuracy, $\sim 1\%$, a pure $Fe^{II}$ (LS) state was observed (top spectrum). Two sets of photo-excitation experiments were carried out: a one-week set with $\lambda = 750$ nm, delivering a rather weak intensity on the sample, $P = 13$ mW/cm$^2$; the second one (3 days) reached $P \cong 30$ mW/cm$^2$ with the cut-off filter $\lambda \geq 665$ nm. The spectra were recorded for successive periods of time ($\sim$ 15 hours in average), showing the progressive onset of the $Fe^{III}$(LS) component.

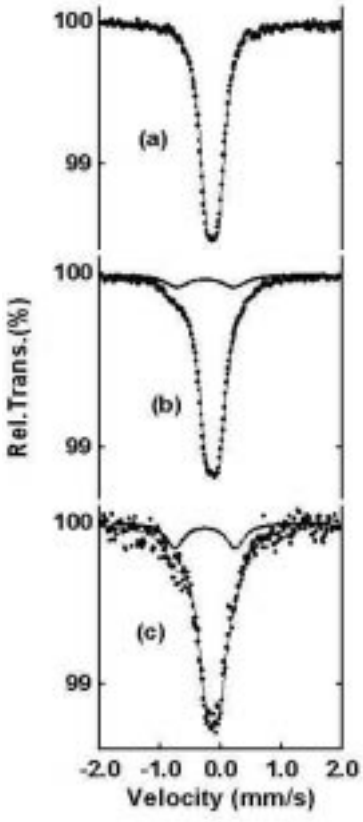


**Fig. 2.** Selected Mössbauer spectra of $Rb_{0.52}Co[Fe(CN)_6]_{0.84}$, 2.3 $H_2O$, polymer-embedded: (a) spectrum before photo-excitation, (b) cumulated spectrum of the best (last) sequences of photo-excitation, for the accurate determination of the spectral components, (c) individual spectrum during the last stage at $P = 30$ mW/cm$^2$ (maximum transformation $\sim 20$ at.%).

**Table 1.** Fitted values of the Mössbauer parameters from the spectra of Figure 2: Isomer shift (IS) is referred to metallic iron at room temperature. QS is the quadrupole splitting, $\Gamma$ the full width of lorentzian lines. Standard deviations of statistical origin are given in brackets. Underlined values were fixed during the fit.

| Spectrum | IS (mm/s) | $\Gamma$ (mm/s) | QS (mm/s) | rel. area (%) |
|---|---|---|---|---|
| a | −0.007(1) | 0.276(2) | 0.190(4) | 100 |
| b | −0.007 | 0.312(4) | 0.190 | 86(1) |
| | −0.126 | 0.494(3) | 0.92(2) | 14(1) |
| c | −0.007 | 0.39(1) | 0.190 | 79(2) |
| | −0.126 | 0.50 | 0.92 | 21(2) |

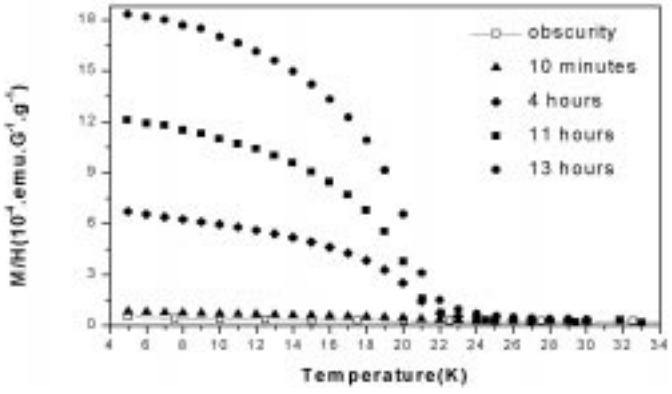


**Fig. 3.** Field-cooled magnetization curves of $Rb_{0.52}Co[Fe(CN)_6]_{0.84}$, 2.3 $H_2O$, measured in $H = 50$ Oe, before and after different irradiation times at $\lambda > 665$ nm, $T = 10$ K, $H = 50$ Oe, $P = 50$ mW/cm$^2$.

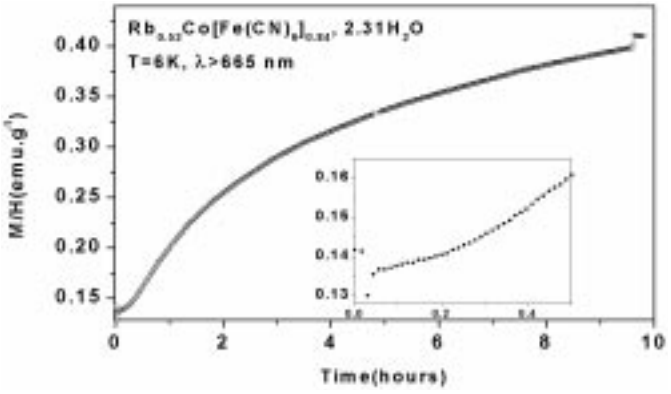


**Fig. 4.** Kinetics of the photo-excitation of $Rb_{0.52}Co[Fe(CN)_6]_{0.84}$, 2.3 $H_2O$, at 6 K, $\lambda > 665$ nm, $p = 50$ mW/cm$^2$. The jump up when the light is switched off reveals a slight warming effect on the sample during the illumination stage. Inserted is a zoom of the initial part of the curve.

The analysis of the spectra consisted in two steps: (i) the accurate fitting of the hyperfine parameter values, by using a "total" spectrum (middle spectrum in Fig. 2), obtained by summing up several spectra selected for their high degree of transformation. The so-determined parameter values of the photo-induced component are very close to those reported in literature for ferricyanides [8], and therefore characterize the ferric state. (ii) then, each individual spectrum was analyzed accurately by fixing the IS, QS values of the spectral components, and thus provided accurately the proportion of the photo-excited state, in spite of the poor statistics (see Fig. 2, bottom, for a typical example of low-statistics individual spectrum). The resulting time dependence will be shown in Figure 5, and discussed further on.

We show in Figure 3 field-cooled (FC) magnetization data recorded in the dark, before and after illumination. The sample is polycrystalline $Rb_{0.52}Co[Fe(CN)_6]_{0.84}$. Before illumination, the magnetization is small, due to few $Co^{II}$ ions, diluted in a diamagnetic matrix. Starting from the same initial state (de-excited after annealing at 150 K for at least 10 minutes), illumination was performed at $T = 10$ K, $\lambda > 665$ nm, $P \cong 50$ mW/cm$^2$. After illumination the FC procedure was carried out in the dark. During the whole experiment (excitation + magnetic annealing at 30 K + measurement) the field was kept constant. The curves are shown for different illumination times, and beyond a short illumination time/some 10 minutes all the curves indicate the same value of the magnetic ordering temperature $\sim$ 21 K. Further experiments have shown that this temperature do not sizably depend on the value of the magnetic field applied during the illumination of the sample.

The quasi-constant value of this photo-induced magnetic ordering temperature reveals an inhomogeneous process, with a photo-induced saturated state, which progressively propagates through the sample, as a function of the illumination time. This is due to the large bulk absorption of light, leading to a frontal propagation of the photo-excited state through the sample, by layers more or less

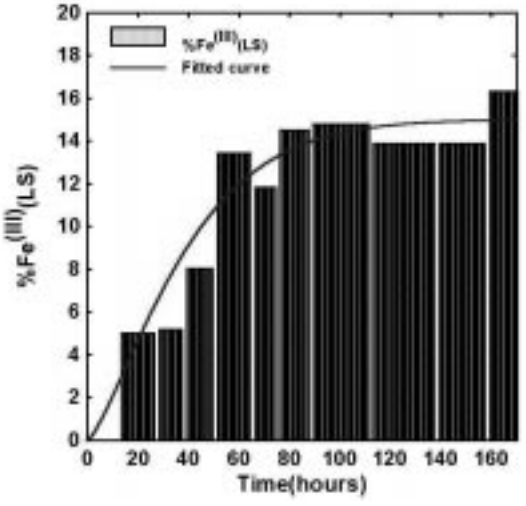


**Fig. 5.** Mössbauer data for the kinetics of photo-excitation of $Rb_{0.52}Co[Fe(CN)_6]_{0.84}$, 2.3 $H_2O$, polymer-embedded, at $T = 45$ K, with $\lambda = 750$ nm, $p = 13$ mW/cm$^2$.

parallel to the surface. Such a frontal process was previously recognized in the case of other photo-excitable systems, such as the spin-crossover complexes, where photo-excitation proceeds by the so-called LIESST effect [9,10]. Let us discuss first the inhomogeneous character of the photo-excitation process.

The inhomogeneous effect is particularly large in the present case because of the high absorbance of the dark-blue material. This severely reduces the intensity of light in the bulk of the material. The bulk attenuation effect [5,10] affects the kinetics of the photo-excitation process. We show in Figure 4 the increase in magnetization, plotted as a function of time: while the incident intensity is kept constant, magnetization increases following a stretched exponential law, consistent with the Mössbauer data which are shown in Figure 5. It is worth remarking a small non-linearity of the magnetization curve (Fig. 4),

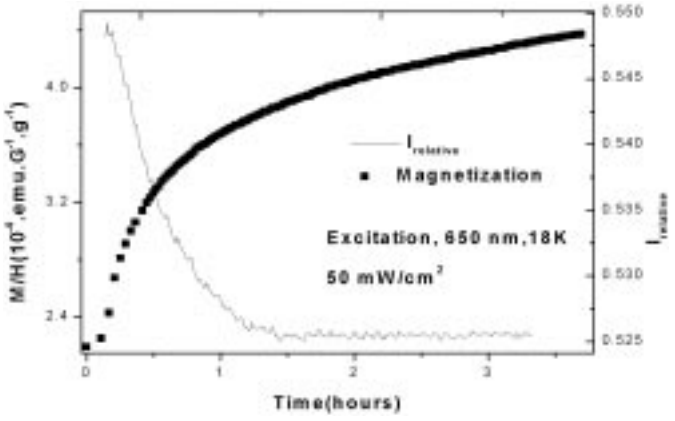


**Fig. 6.** Magnetic and reflectivity data for the kinetics of photo-excitation of $Rb_{0.52}Co[Fe(CN)_6]_{0.84}$, 2.3 $H_2O$, polycrystalline, $H = 100$ Oe, $T = 18$ K, $\lambda = 650$ nm, $P = 50$ mW/cm$^2$. The reflectivity scale has been matched to the magnetic scale.

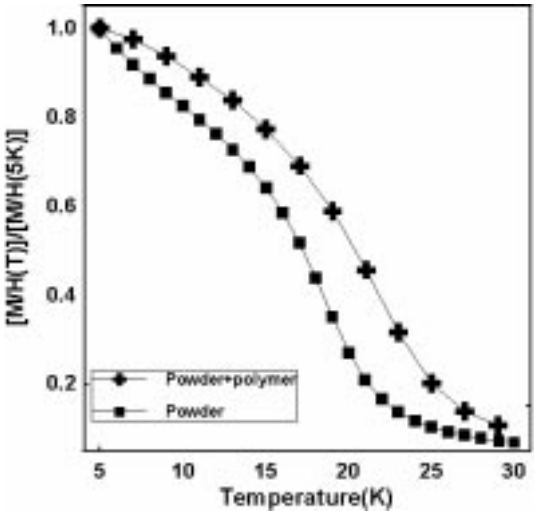


**Fig. 7.** Field-cooled magnetization curves ($H = 100$ Oe) after photo-excitation at $\lambda = 750$ nm, $P = 50$ mW/cm$^2$, $t = 10$ h: polycrystalline sample ($T_C \sim 20$ K) and the corresponding polymer-embedded sample ($T_C \sim 26$ K). Vertical scale was normalized to the same $M(T = 5$ K). $T_C$ is determined here from the intersect of the maximum slope line and the baseline.

at the beginning of the photo-excitation process. It is better seen in low-intensity measurements (Fig. 3 of Ref. [3]). We explain it as due to the non-linear response of the unsaturated part of the sample, while both the magnetic moments and the interactions built up at low temperature.

We report in Figure 6 a clear confirmation of the frontal character of the process, by comparing the magnetization and reflectivity signals, simultaneously recorded [3,5]. While the reflected intensity rapidly saturates, the magnetic signal keeps increasing, showing that the bulk is obviously far from saturation. Repeated experiments on a given sample, after the thermal annealing which returns the sample to its stable electronic state, always gave reproducible $T_C$ values. Also, the $T_C$ data for different polycrystalline samples were spread from 20–21 K and reached 26 K for the polymer-embedded sample (Fig. 7). This spread was probably due to slight differences in stoichiometry. The stoichiometry departure was presumably larger in the polymer-embedded sample, for which the chemical analysis was no longer possible, and we did not investigate further the probable relationship between stoichiometry and Curie temperature. However, the values reported here have enabled us to conclude that the character of the light-induced transformation described by equation (2) is achieved to a rather large extent. Indeed, the expected $T_C$ value can be estimated by comparison to the well-documented case of $Co_3Fe_2$, representative of the ideal ferrimagnetic case with 3:2 structure, and for which $T_C = 15$ K [11]. For such a comparison we only consider the dominant A-B interaction, in mean-field approach, with a complete Co sub-lattice (A) and an incomplete Fe sub-lattice (B). Then $T_C$ is proportional to the coupling constant $|J|$ and to the number $z$ of Fe neighbors around the Co atoms, *i.e.* $T_C \propto z|J|$. Assuming an identical $J$-value in both systems, with $z = 4$ for $Co_3Fe_2$ and $z = 6$ for ideal RbCoFe, it comes $T_C(\text{RbCoFe})/T_C(Co_3Fe_2) = 1.5$; with the experimental stoichiometry $CoFe_{0.84}$, it comes $z = 5$ and the $T_C$ ratio 1.25 which reasonably fits the experimental ratio 21 K/15 K = 1.4.

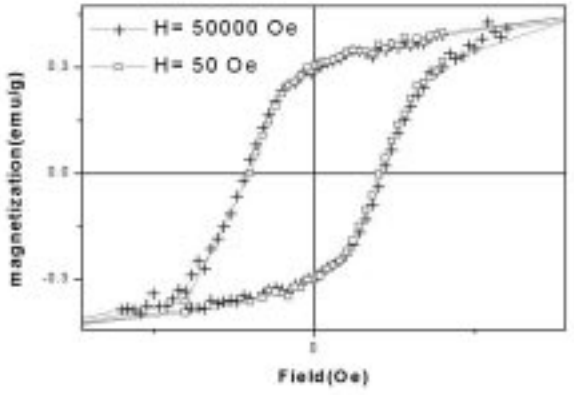


**Fig. 8.** $B - H$ loops of $Rb_{0.52}Co[Fe(CN)_6]_{0.84}$, 2.3 at 10 K, recorded after photo-excitation under different magnetic fields.

Quantitative estimates of the transformed fraction of the material are interesting since they reveal the efficiency of the various photo-excitation devices. In Mössbauer experiments, no more than $\sim 20$ at.% were transformed. In the SQUID experiments, due to the large parasitic contributions of the optical device, we had to estimate this fraction from the decrease in magnetization during the thermal decay (the latter will be shown in Fig. 10); assuming a Curie law, the fraction was estimated to be $\sim 14 \pm 3\%$ in the best case.

We also have tested the efficiency of the photo-excitation process under various experimental conditions, each time starting from the de-excited state, and applying illumination during equal times. We thus investigated the effect of:

(i) temperature: up to 60 K, the efficiency of the photo-excitation process remains $\sim$ constant. It decreases

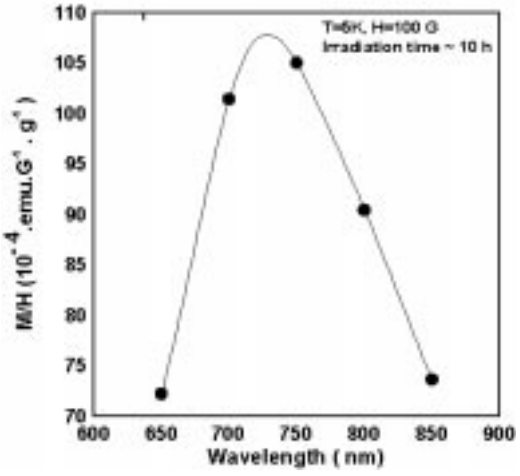


**Fig. 9.** Spectral analysis of the photo-excitation of $Rb_{0.52}Co[Fe(CN)_6]_{0.84}$, 2.3 $H_2O$, after 10 h irradiation at 5 K, 100 Oe, using different wavelengths: the FC magnetization is plotted *vs.* $\lambda$. The solid line is a guide for the eye.

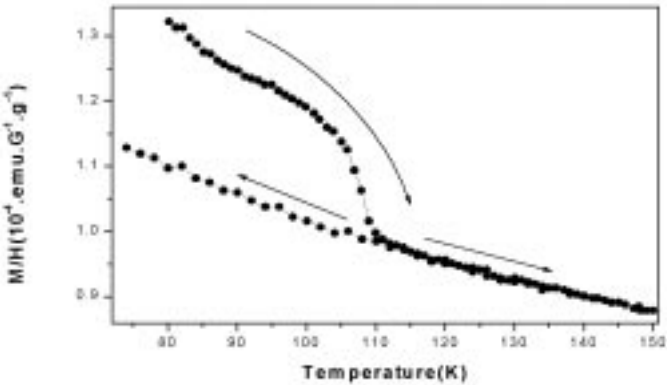


**Fig. 10.** Magnetic data for the thermal decay, in the dark, of the electronic excited state of $Rb_{0.52}Co[Fe(CN)_6]_{0.84}$, 2.3 $H_2O$, created by illumination at $\lambda > 665$ nm, $P = 60$ mW/cm$^2$, $t = 18$ h. The up-going curve is that of the excited electronic state, the down-going is that of the de-excited state, which approximately superimposes the one of the non-excited state. The temperature sweeping rate is typically: 0.3 K/min.

by a factor $\sim 0.5$ at 75 K and drops to $\sim 0$ at 90 K [12]. This obviously is due to the thermal activation of the relaxation process, which is analyzed in the next section;

(ii) magnetic field: the $B - H$ loops recorded at 10 K after photo-excitation under different fields (Fig. 8) are quasi identical, and thus indicate that the photo-excitation is not sizably field-sensitive;

(iii) wavelength: different optical filters have been used, with all other conditions identical. The data are displayed in Figure 9, showing that the photo-excitation process is efficient in a broad range of wavelengths, at the red edge of the visible domain. The optimum value, with the present photo-excitation device, is around 700–750 nm. At 448 nm (argon laser) the reverse process was observed [12], but much slower, probably because of the larger optical density at short wavelength.

The occurrence of photo-excitation over a large $\lambda$ – interval is obviously related to the lack of structure of the optical absorption spectrum of the bimetallic cyanides. Such optical properties highly contrast with those of spin-crossover complexes, the sharp lines of which provide an easy optical characterization of the spin states, as well as a rapid switching of these states by the direct and reverse LIESST effects [13].

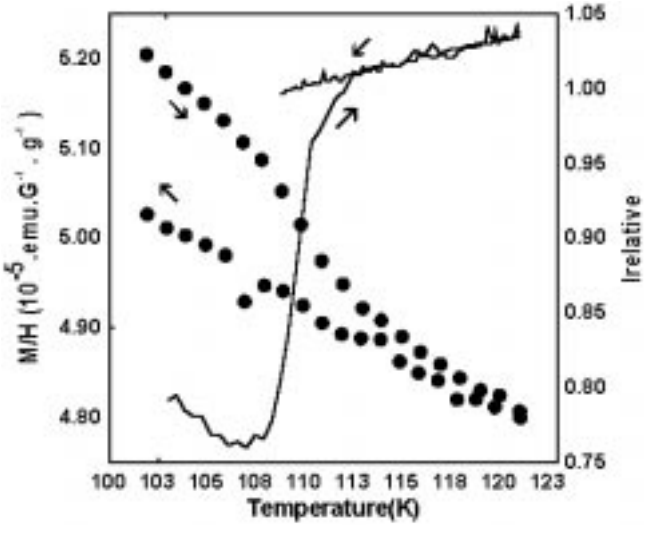


**Fig. 11.** Simultaneous magnetic (dots) and reflectivity (line) data for the thermal decay of the electronic excited state of $Rb_{0.52}Co[Fe(CN)_6]_{0.84}$, 2.3 $H_2O$, created by illumination at $\lambda = 750$ nm, $P = 20$ mW/cm$^2$, $t = 1$ h. The reflectivity scale has been matched to the magnetic scale. Both techniques indicate the onset of de-excitation at $\sim 110$ K (for the sweeping rate: 0.3 K/min). Note the sensitivity of the reflectivity detection, useful in the present case of a weak photo-excitation.

## 4 Electronic relaxation

We observed the decay of the excited electronic state, by warming the sample up to 150 K, at the temperature sweeping rate $\sim 0.3$ K min$^{-1}$. This is shown in Figure 10 for the magnetization recorded in the dark, and in Figure 11 for the coupled magnetization/reflectivity measurement. The decay is observed in Figure 10 at $\sim 110$ K, merely resulting in a rather sharp (irreversible) drop of the magnetization. In Figure 11 the presence of light, $\lambda = 750$ nm, $P = 20$ mW/cm$^2$, slightly affects the decay, by a small temperature shift probably associated with the local warming of the surface of the sample. The reflectivity signal increased during the decay, at the reverse of during the photo-excitation (see Fig. 6).

We started investigating the kinetics of the thermal relaxation, in the dark, at the constant temperature of 95 K. The curve is plotted in Figure 12. We describe the curve as made of two parts, probably associated with a

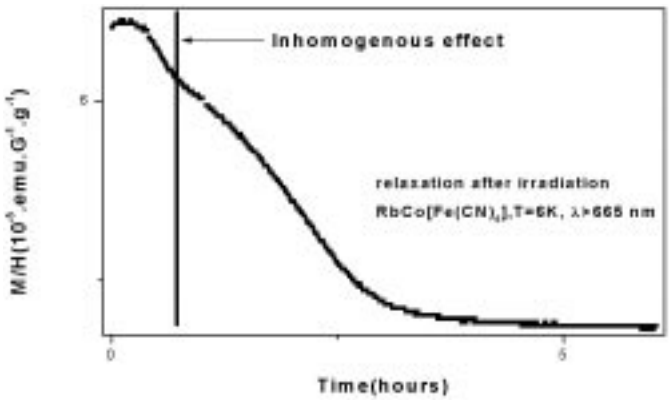


**Fig. 12.** De-excitation at 95 K, in the dark, of $Rb_{0.52}Co[Fe(CN)_6]_{0.84}$, 2.3 $H_2O$, after photo-excitation at $T = 18$ K, $t = 10$ h, $\lambda = 750$ nm, $P = 50$ mW/cm$^2$.

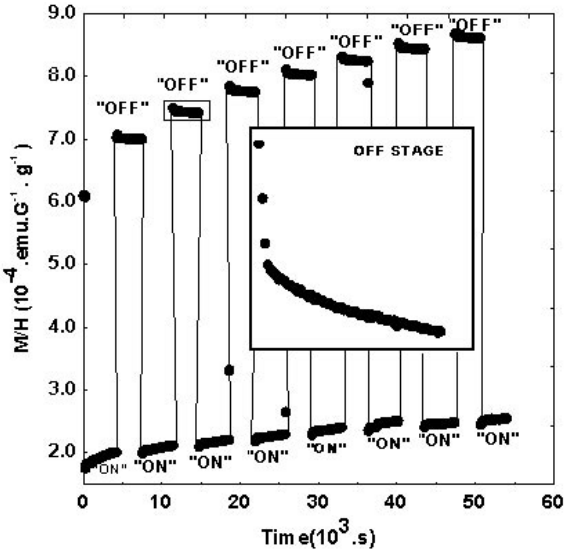


**Fig. 13.** Magnetization of $Rb_{0.52}Co[Fe(CN)_6]_{0.84}$, 2.3 $H_2O$, under chopped light at $T = 20$ K, $\lambda = 750$ nm, $P = 40$ mW/cm$^2$. The light was set alternatively *on* and *off*. The reversible jumps in magnetization are due to the warming effect of light (see text). The ascending parts are due to the effect of the photo-excitation process. We focus here on the repeated decrease in magnetization, at each off-stage, explained as the decay of the front layer of the photo-excited zone. The insert is a zoom of the framed off-stage curve. The initial drop is due to the transient regime of heat conduction in the sample; the further decrease then gives evidence for the relaxation of the metastable photo-excited state.

structural inhomogeneity of the material. Clearly the major part of the curve follows a non-exponential law, with a sigmoidal shape typical for a self-accelerated process, already analyzed in the case of the spin transitions, as due to cooperative effects on the relaxation rate [14]. The self-acceleration is explained by a progressive lowering of the energy barrier of the metastable state associated with the depopulation of this state. In other words, the lifetime of the excited state is an increasing function of the degree of photo-excitation. Thus the first part of the curve should be attributed to the sample areas the more departing from the ideal stoichiometry.

Such a cooperative effect on the energy barrier plays a crucial role at the very beginning of the photo-excitation process: the first excited Co–Fe pairs have a very short lifetime. Consequently, the photo-excitation process has to be fast enough to provide a sufficient population of the excited state, which ensures the raising up of the energy barrier (this effect results in an intensity threshold described in [15]). Then, only the saturated parts of the sample have a long lifetime and therefore remain populated at higher temperatures, till the thermal decay is observed.

For better investigating the first steps of the photo-excitation process, we used a chopped light of weak intensity. Temperature was raised near the Curie temperature of the saturated material, in order to avoid the magnetic irreversibilities which will be discussed in the next section, and also to obtain a quasi-linear response of the magnetic signal to the number of excited pairs. The temperature and field were kept constant, the light was alternatively switched on and off, and the magnetization was recorded as a function of time (Fig. 13). The data reveal several typical features:

(i) a large magnetization increase upon the first stage of illumination, followed by smaller and smaller increases (stages "on"); this agrees with the stretched exponential curve previously shown in Figures 4 and 5;

(ii) reversible jumps occurring when the light is switched on and off, which are due to a purely thermal effect on the sample; these magnetization jumps due to the thermal effect are particularly large because temperature was close to the Curie temperature;

(iii) small decreases similarly occurring after each illumination stage, which reveal the rapid decay of a small proportion of the photo-excited pairs.

The repeated character of this decay can be explained by combining the inhomogeneous (frontal) character of the photo-excitation process and the dependence of the relaxation rate upon the local degree of transformation of the material: at each "on" stage (illumination), an unsaturated frontier zone is created, which relaxes rapidly during the following "off" stage (in the dark). Under illumination, the frontier zone propagates through the material, and the kinetics of the photo-excitation process finally reduces to the frontal propagation of the saturated phase, with a thin unsaturated, short-lifetimed, frontier layer. Thus the time dependencies observed in the magnetic and Mössbauer data of Figures 4–6 just measure the slower and slower progression of the frontier layer in the sample.

In Figure 14, we show the relaxation effect, observed again at low temperature, over a longer time. The non-exponential shape, already suggested by the small decreasing curves in Figure 13, is confirmed. The stretched

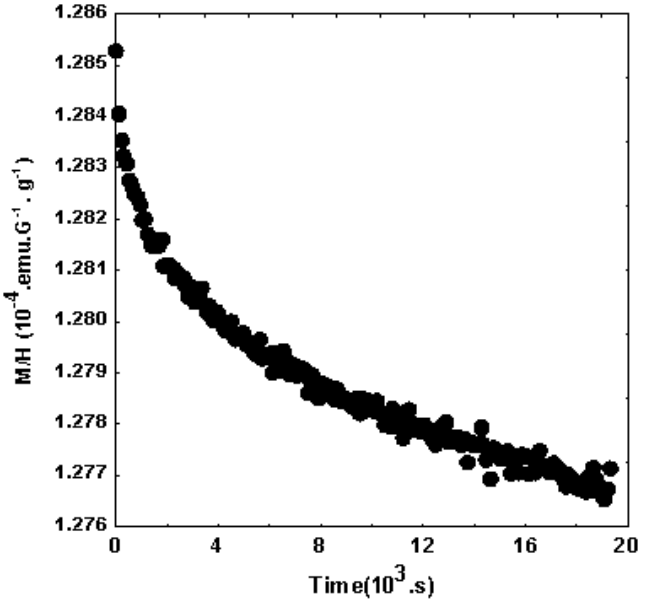


**Fig. 14.** Relaxation of photo-excited $Rb_{0.52}Co[Fe(CN)_6]_{0.84}$, 2.3 $H_2O$. The magnetization is measured at $T = 25$ K after photo-excitation at $\lambda = 750$ nm, $P = 40$ mW/cm$^2$, $T = 10$ K, $t = 10$ h.

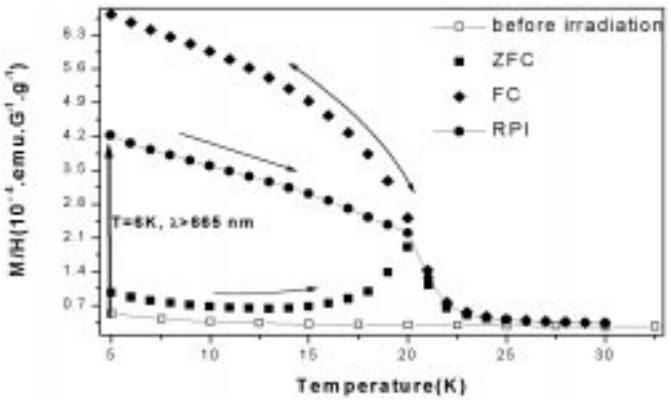


**Fig. 15.** Magnetic metastability of photo-excited $Rb_{0.52}Co[Fe(CN)_6]_{0.84}$, 2.3 $H_2O$, after illumination at $T = 5$ K, $H = 50$ Oe, $t = 12$ h, $\lambda > 665$ nm, $P = 3$ mW/cm$^2$. The 4 magnetization curves have been recorded in the dark, under permanent field, with the following sequence: non-excited state (bottom curve); the up-going curve of the metastable Raw Photo-Induced state (RPI) obtained just after illumination; the reversible Field-Cooled (FC) curve, obtained after annealing at 30 K. For comparison the corresponding Zero-Field Cooled (ZFC) curve has been recorded (the photo-excited sample was annealed at 30 K and cooled down to 5 K in absence of magnetic field before proceeding to the magnetization measurements with increasing temperatures).

exponential shape reveals a distribution of relaxation times. Knowing the dependence of the relaxation time upon the degree of excitation, this distribution is easily attributed to the inhomogeneous degree of excitation, which continuously increases from the front side to the rear side of the frontier layer.

Although this inhomogeneous character of the relaxation seems now well-documented, its actual mechanism may be not definitively established.

## 5 Magnetic properties of the photo-induced state

When the photo-excitation process is performed at low temperature (*e.g.* 10 K), under weak magnetic field (*e.g.* 50 Oe) and moderate light intensity (few mW/cm$^2$), the resulting magnetic state reveals a metastable character, with a thermal magnetization curve in-between the field-cooled (FC) and zero-field cooled (ZFC) curves. The FC and ZFC curves, as usual for non-aging magnetic materials, could be repeated several times, at will. On the contrary, the metastable magnetic state was lost as soon as a FC or ZFC (or a B-H loop) curve was processed. Such a state immediately following the photo-excitation process is therefore denoted the Raw Photo-Induced State (RPI).

The curves are shown in Figure 15. After cooling in the dark, the sample is photo-excited at 5 K, at low intensity in order to reduce the warming effect, for a rather long time (typically over night). Then, the light is switched off and temperature is increased. The system first follows the RPI curve. After annealing at $T_C$, it reversibly follows the FC curve, thus establishing the metastable character of the RPI state. We show in Figure 16 how the magnetization curve, under constant field, progressively shifts towards the FC curve, during a set of successive annealing closer and closer to $T_C$.

Further experiments showed the RPI state is only obtained in low external fields (below $\sim 100$ Oe), and suggest irreversibility mechanisms in terms of domain structure and coercive field, rather than in terms of a frustrated magnetic structure.

## 6 Discussion

Cobalt hexacyanoferrate based compounds exhibit photo-excitation properties of a novel class of magnetic materials. The concentration of magnetic ions can be controlled, reversibly in principle, by the light, an external parameter easy to tune and to switch.

These photo-induced magnetic systems inherently possess a double metastability, electronic and magnetic. However these two aspects are essentially different, since the magnetic metastability involves energies several orders of magnitude smaller than the electronic one. Therefore the photo-excitation (electronic in nature) was expected to be little sensitive to external magnetic fields, as well as to the magnetic state of the material. At the reverse, the magnetic properties reflect all the thermo-photo-magnetic history of the sample.

Magnetic metastability occurs as a result of the photo-excitation, with a RPI state resulting from a peculiar building process of the magnetic system, the magnetic

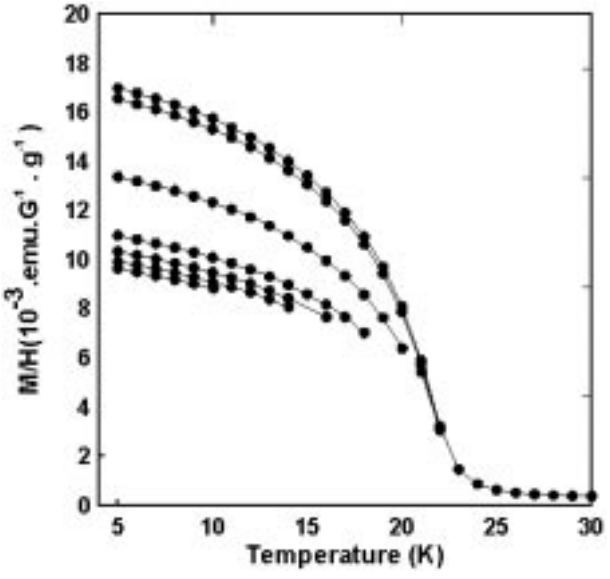


**Fig. 16.** Magnetic metastability of the RPI state of $Rb_{0.52}Co[Fe(CN)_6]_{0.84}$, 2.3 $H_2O$, after photo-excitation at $T =$ 10 K, $H = 50$ Oe, $t = 10$ h, $\lambda = 750$ nm, $P = 3$ mW/cm$^2$: the irreversible evolution of the RPI state towards the FC state, is shown upon successive annealing stages on increasing temperature with the following values: [5 → 10 K]; [5 → 14 K]; [5 → 16 K]; [5 → 18 K]; [5 → 20 K]; [5 → 22 K]; the top curve is FC (annealed at 30 K).

moments of which have been created below $T_C$. At such a low temperature the thermal relaxation of the magnetic system is not efficient enough to ensure the thermal equilibrium of the system. Indeed, we have once proceeded to a rapid cooling of the sample, from 30 K down to 5 K, and we could observe a magnetisation curve close to the initial RPI curve. In the limiting case of totally frozen magnetic moments, the magnetic structure would be highly frustrated, spin-glass-like.

No doubt that these systems will provide, not only a wealth of metastable situations, but also diluted systems in unprecedented experimental conditions, of basic interest for the magnetism of disordered and spin-glass like systems.

However, the development of such investigations has to face the crucial problem of the optical density. This should promote the preparation of thin layer samples, or the use of optical and magneto-optical measuring devices. It is worth noting that the variation of the reflected intensity during the excitation process seems to be the reverse of the simple bleaching effect which is expected from the simplest considerations, and which works fine in the case of spin transitions [13]: the removal of absorbing centers reduces the optical absorption of the sample, and hence increases the reflected intensity. The present situation (photo-darkening?) is obviously more complex, due to the prominent intermetallic charge transfer transitions.

The relatively high value of the temperature range where the thermal decay to the ground state occurs ∼ 110 K, is encouraging with respect to the spin transition compounds, for which the corresponding range is 60–70 K for most of the examples (the thermal relaxation of the LIESST effect could however be observed at a comparable time scale, up to 180 K, on an example of nickel-diluted spin-crossover complexes [18]). The actual characteristics of the energy barrier responsible for such a long lifetime have to be determined. They can be investigated through a detailed study of the relaxation curves as a function of temperature, and of the related changes in the structure. We think that the change in the spin state of the cobalt ion, associated with a change in the Co–N distances [16], is the cornerstone of the problem, like in the spin transition complexes [17].

## 7 Conclusion

We have shown, in the cobalt ferrocyanide, a photo-induced transformation from dia- to ferri-magnetism, which is almost complete. Some aspects of the photo-excitation mechanism have been elucidated, namely the frontal character of the process and the antagonistic role of a non-linear relaxation during the crucial first steps of the process. The double metastability, electronic and magnetic, has been described for the first time, and should apply as well to all magnetic structures photo-induced at low temperatures.

Drs. M. Noguès and E. Codjovi are acknowledged for precious help during the photomagnetic measurements, Mrs A. Wack and P. Renaudin for technical support, Drs J. Jeftic and J.L. Dormann for stimulating discussions, Prof. G. Férey for a Ph.D. grant to O.R. Financial support was given by CNRS and by European Communities: Action COST No. 518, Contract TMR/TOSS (FMRX-CT98-0199), Contract TMR/3MD (ERBFM-RXCT980181).

## References

1. S. Ferlay, T. Mallah, R. Ouahès, P. Veillet, M. Verdaguer, Nature **378**, 701 (1995).
2. O. Sato, T. Iyoda, A. Fujishima, K. Hashimoto, Science **272**, 704 (1996); O. Sato, Y. Einaga, T. Iyoda, A. Fujishima, K. Hashimoto, J. Electrochem. Soc. **144**, L11 (1997); Y. Einaga, O. Sato, T. Iyoda, Y. Kobayashi, F. Ambe, K. Hashimoto, A. Fujishima, Chem. Lett. **4**, 289 (1997).
3. F. Varret, H. Constant-Machado, J.L. Dormann, A. Goujon, J. Jeftic, M. Noguès, A. Bousseksou, S. Klokishner, A. Dolbecq, M. Verdaguer, *ICAME'97, Intern. Conf. on Applic. of the Mössbauer Effect* (Rio de Janeiro, Sept. 1997), Proceedings in Hyperf. Inter. **113**, 37 (1998).
4. A. Bleuzen, C. Lomenech, A. Dolbecq, F. Villain, A. Goujon, O. Roubeau, M. Noguès, F. Varret, F. Baudelet, E. Dartyge, C. Giorgetti, J. Gallet, C. Cartier, M. Verdaguer *ICMM'98* (Seignosse, France), Proceedings in J. Mol. Cryst. Liq. Cryst. **335**, 965 (1999).
5. E. Codjovi , W. Morscheidt, J. Jeftic, J. Linares, M. Nogues, A. Goujon, O. Roubeau, H. Constant-Machado,

A. Desaix, A. Bousseksou, M. Verdaguer, F.Varret, *ICMM'98* (Seignosse, France), Proceedings in J. Mol. Cryst. Liq. Cryst. **335**, 1295 (1999).
6. P. Tran-Van *et al.*, C. R. Acad. Sci. Ser. B (submitted).
7. W. Morscheidt, E. Codjovi, J. Jeftic, A. Bousseksou, J. Linarès, F. Varret, Measurement Sci. Technol. **9**, 1311 (1998).
8. N.N. Greenwood, T.C. Gibb, in *Mössbauer Spectroscopy* (Champan and Hall, London, 1971), pp. 169-187.
9. S. Decurtins, P. Gütlich, H. Spiering, A. Hauser, Inorg. Chem. **24**, 2174 (1985).
10. A. Hauser, Chem. Phys. Lett. **124**, 5438 (1986).
11. M. Verdaguer, T. Mallah, V. Gadet, I. Castro, C. Hèlary, S. Thiébaut, P. Veillet, *Contributions to Development of Coordination Chemistry*, edited by G. Ondrejovic, A. Sirota (Slovak Technical University Press, Bratislava, 1993), pp. 19–24.
12. A. Goujon, rapport de DEA, Versailles, 1997.
13. A. Hauser, Comments Inorg. Chem. **17**, 17 (1995).
14. T. Buchen, P. Gütlich, H.A. Goodwin, Inorg. Chem. **33**, 4573 (1994); A. Hauser, Chem. Phys. Lett. **192**, 65 (1992).
15. A. Desaix, O. Roubeau, J. Jeftic, J. Haasnoot, K. Boukheddaden, E. Codjovi, J. Linarès, M. Noguès, F. Varret, Eur. Phys. J. B **6**, 183 (1998).
16. A. Bleuzen, C. Cartier, F. Villain, work in progress at LURE, the French Synchrotron Radiation Facility.
17. O. Kahn, *Molecular Magnetism* (VCH, New York, 1993); E. König, Structure and Bonding **76**, 51 (1991); P. Gütlich, A. Hauser, H. Spiering, Angew. Chem. Int. Ed. Engl. **33**, 2024 (1994).
18. Th. Buchen, P. Gütlich, *Second Europ. Inorg. Chem. Seminar Wiesbaden, April 16-20 1990*, p. 56; Th. Buchen, D. Schollmeyer, P. Güetlich, Inorg. Chem. **35**, 155 (1996).